Chapter 10.1

Acid Activation of Clay Minerals

P. Komadel and J. Madejová
Institute of Inorganic Chemistry, Slovak Academy of Sciences, Bratislava, Slovakia

Chapter Outline

One of the most common chemical modifications of clay minerals, used for both industrial and scientific purposes, is their acid activation. This consists of the reaction of clay minerals with a mineral acid solution, usually HCl or H_2SO_4. The main task is to obtain partly dissolved material of increased specific surface area (SSA), porosity and surface acidity (Komadel, 2003; Carrado and Komadel, 2009). The manufactured materials are widely available, relatively inexpensive solid sources of protons, and effective in a number of industrially significant reactions and processes. Acid attack on clay minerals also occurs naturally, for example, in the interaction of acid mine drainage with clay minerals (Galán et al., 1999; Dubíková et al., 2002). Mining waste containing sulphides is the most common and the greatest anthropogenic source of acidity. Progressive oxidation leads to the production of protons and sulphates in leaching waters, which generally also mobilize large amounts of metals by dissolution of minerals. These waters influence the composition of

Developments in Clay Science, Vol. 5A. http://dx.doi.org/10.1016/B978-0-08-098258-8.00013-4

surface waters but also have an impact on surrounding soils and terrestrial ecosystems.

Upon acid treatment, protons penetrate into the mineral layers and attack the structural OH groups. The resulting dehydroxylation is connected with the successive release of the central atoms from the octahedra as well as with the removal of Al from the tetrahedral sheets. Simultaneously, a gradual transformation of the tetrahedral sheets into a three-dimensional framework proceeds. Depending on the extent of acid activation, the resulting solid product contains unaltered layers and amorphous silica, while the ambient acid solution contains ions according to the chemical composition of the clay mineral and the acid used. The final reaction product of various acid-treated clay minerals is always the same. For several silicates, such as trioctahedral smectites (Vicente et al., 1995a; Komadel et al., 1996b), dioctahedral smectites (Komadel et al., 1990; Tkáč et al., 1994; He et al., 2002), illite-smectite (Pentrák et al., 2010), sepiolite (Vicente et al., 1995b) and palygorskite (Suárez Barrios et al., 1995), this product consists of amorphous, porous, protonated and hydrated silica with a three-dimensional cross-linked structure (Komadel, 1999).

From the industrial point of view, the term 'acid-activated clays' was reserved mainly for partly dissolved bentonites. Bentonite has always had a multitude of markets, and acid-activated bentonite has been a traditional product for many decades. It is usually a Ca^{2+}-bentonite that is treated with inorganic acids to replace divalent calcium ions with monovalent hydrogen ions and to leach out ferric, ferrous, aluminium, and magnesium ions, thus altering the layers of smectite and increasing the SSA and porosity. This results in the production of bleaching earths, that is, clays suitable for a range of bleaching or decolourizing applications, in which they compete against natural bleaching earths (Siddiqui, 1968; Kendall, 1996; Christidis et al., 1997; Falaras et al., 1999; Hussin et al., 2011).

This chapter mainly reviews acid treatment of smectites, which are the dominant minerals in bentonites. Other products include environmentally benign catalysts or their supports, which are used in various chemical reactions such as Friedel–Crafts alkylation and acylation, dimerization and polymerization of unsaturated hydrocarbons (Adams, 1987; Brown, 1994), or as colour developers in carbonless copying papers (Fahn and Fenderl, 1983). Acid-treated clay minerals pillared with (hydr)oxy aluminium species are used to prepare clay mineral-modified electrodes (Falaras et al., 2000a), as adsorbents for oil clarification (Mokaya et al., 1993; Falaras et al., 2000b; Pagano et al., 2001), and as catalysts (Mokaya and Jones, 1994; Bovey and Jones, 1995; Bovey et al., 1996).

10.1.1 METHODS OF INVESTIGATION

The methods being employed to characterize the acid-activated silicates include chemical analysis; X-ray diffraction (XRD); Mössbauer, Fourier transform infrared (FTIR), and magic angle spinning nuclear magnetic

resonance (MAS-NMR) spectroscopies; scanning (SEM), transmission (TEM), and high-resolution transmission electron microscopies (HRTEM); and acidity, surface area, and pore-size measurements. Usually, a combination of several methods is needed for sufficient characterization of the materials obtained (Čičel and Komadel, 1994; Vicente et al., 1994, 1996b; Breen et al., 1995b; Komadel et al., 1996b; Gates et al., 2002; Klika et al., 2011; Scarletti et al., 2011; Ramesh et al., 2012).

Chemical analyses of solid and/or liquid reaction products and MAS-NMR and IR spectroscopies are very sensitive to the nature and content of the octahedral atoms and thus also to the changes that occur in different stages of acid attack (Breen et al., 1995a,b). The extent of dissolution of different chemical components of the sample can be determined by chemical analysis of the starting material and by analysis of the acid solutions reacted for specified times. The filtrate and washing solutions are combined and usually analyzed by atomic absorption spectroscopy (Pentrák et al., 2010).

Spectroscopy in the mid-IR (MIR) region is a routine characterization technique for acid-treated clay minerals. As protons penetrate into the clay mineral layers and attack the OH groups, the resulting dehydroxylation connected with the successive release of the octahedral atoms can be readily followed by changes in the characteristic absorption bands attributed to vibrations of OH groups and/or octahedral cations. Comparative IR studies of acid-treated smectites (Madejová et al., 1998) as well as saponites, sepiolite and palygorskite (Vicente et al., 1996a) have been published.

In addition to the spectra obtained in the MIR region, the spectra measured in the near-infrared (NIR) region can provide useful information about the decomposition of clay minerals in inorganic acids since the observed bands related to the vibrations of OH groups are sensitively affected by the variations in the mineral structure. However, despite the non-destructive character of NIR spectroscopy and the simplicity of sample preparation, its utilization for acid-treated clay minerals remains rather rare (Madejová et al., 2007, 2009a; Pentrák et al., 2009, 2010; Tomić et al., 2012).

10.1.2 H^+-EXCHANGED CLAY MINERALS

The acidity of acid-untreated smectites has two sources: (i) the compensating cations, which may have a strong polarizing effect on coordinating water molecules, most of which are in the interlayer spaces and may not be easily accessible and (ii) specific sites at the layer edges, which may be compensated by OH group formation, leading to Brønsted acid sites such as Si–OH. Also, coordinatively unsaturated Al^{3+} and Mg^{2+} are easily formed at the edges and act as Lewis acid sites (Lambert and Poncelet, 1997).

The first step during acid treatment is that the protons replace the exchangeable cations; then they attack the layers (Čičel and Komadel, 1994). The exchange reaction was fast if there was good contact between

the acid and smectite and the quantity of available protons was sufficient. The substitution rate was independent of the smectite if the clay mineral contained only swelling layers. In contrast to smectites saturated with metal cations, proton-saturated smectites were unstable. The layers were attacked by surface and interlayer hydrated protons, even after drying the separated activated smectite, similar to what occurred in solution. This process, known as 'auto-transformation', spontaneously changed H^+-smectites to their Al^{3+}, Fe^{3+}, or Mg^{2+} forms on ageing (Barshad and Foscolos, 1970). In aqueous dispersion at 90 °C, the process was completed within 4 days (Janek and Komadel, 1999).

To study the properties of H^+-clay minerals, maximal saturation by protons and stability of the product were required. Various preparation methods were tested. The best results were obtained by passing the clay dispersion through a succession of H^+, OH^- and H^+ ion-exchange resins. H^+-forms of <2 μm fractions of bentonites with various Fe^{3+} contents were prepared by this method. Potentiometric titrations of proton-saturated fine fractions of bentonites were used to characterize the acid sites at the smectite–water interface in dispersions. The titration curves revealed that the number of strong acid sites varied and accounted for 60–95% of the total acidity in the freshly prepared H^+-forms (Janek et al., 1997). Layer-charge (LC) distributions of all samples were inhomogeneous. This distribution changed after oxalate pre-treatment of the samples, due to the removal of readily soluble phases that might have blocked exchange sites. After auto-transformation, the alkylammonium exchange method (Lagaly, 1994) revealed inhomogeneous charge density distributions; the fraction of layers of the highest charge decreased. Comparison of the cation exchange capacity (CEC) obtained from potentiometric curves and the CEC calculated from the mean LC confirmed that the attack of protons occurred from the particle edges. However, for several samples the structural attack may also occur from the interlayer space. Auto-transformation of the H^+-smectites also decreased the mean LC. Protons preferentially attacked the octahedral Mg^{2+} during the auto-transformation. The number of strong acid sites decreased and the number of weak acid sites increased on ageing.

The titration data obtained were used in a thermodynamic calculation of proton affinity distribution. Numerical solution of an integral adsorption equation revealed a continuous distribution of proton interaction sites. Proton affinity distributions clearly detected up to five different proton interaction sites in all the smectite–water systems, within the accessible experimental range of pH between 2 and 12. The amount of the strongest acid sites decreased on ageing, while the amount of all weaker acid sites increased with the progress of auto-transformation. The strongest acid sites were connected with free protons present in the dispersion, while the weaker acid sites were connected with the titration of released structural Al^{3+}, Fe^{3+}, Mg^{2+} cations and/or their hydrolyzed species and deprotonation of SiOH groups. These results indicated the sources of acidity in acid-activated bentonites (Janek

and Komadel, 1993). Hydrated aluminium ions in fresh proton-saturated dispersions contributed to a group of weak acid sites, which also included oligomeric hydroxoaluminum cations. The number of these sites increased during auto-transformation. Freshly prepared proton-saturated dispersions showed low pH values and the particles interacted by edge-to-face contacts. This increased the viscosity in comparison with the sodium forms at pH close to 7 (Janek and Lagaly, 2001). A kinetic study of proton-promoted dissolution of K^+-Mt in solutions with constant KCl concentrations, using both titration and batch equilibration experiments, showed that adsorption of protons and dissolution of Al^{3+} occurred (Zysset and Schindler, 1996).

10.1.3 ACID DISSOLUTION OF SMECTITES

Acid treatment of clay minerals with strong inorganic acids resulted in solid products containing unaltered layers and amorphous three-dimensional cross-linked silica, depending on the extent of acid activation. The IR spectra of SWy-1 montmorillonite (SWy-1 Mt) after reaction with 6 M HCl (Fig. 10.1.1) demonstrated the changes of the chemical bonds in the Mt structure. The gradual decrease in the intensities of the OH bending (930–800 cm^{-1}) and Al–O–Si (524 cm^{-1}) bands indicated the decomposition of the octahedral sheets. Changes in the tetrahedral sheets were reflected in the position and shape of the Si–O stretching band. In addition to the tetrahedral Si–O band near 1048 cm^{-1}, the MIR spectra of the acid-treated samples

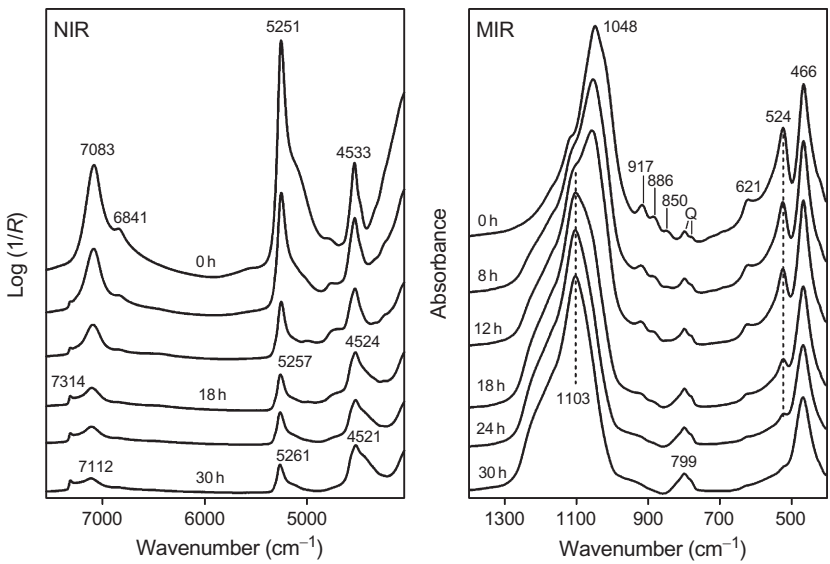

FIGURE 10.1.1 NIR and MIR spectra of SWy-1 Mt treated with 6 M HCl at 95 °C for 0, 8, 12, 18 and 30 h. Q is quartz. *MIR spectra from Madejová et al. (1998).*

revealed a pronounced absorption near 1100 cm^{-1} assigned to Si–O vibrations of amorphous silica with a three-dimensional framework formed during acid treatment. The position of the Si–O band at 1103 cm^{-1} together with the weak inflection near 524 cm^{-1} observed for the sample dissolved for 30 h reflected a very high yet incomplete dissolution of Mt in 6 M HCl (Madejová et al., 1998). NIR spectrum of SWy-1 Mt presented a broad, complex band at 7083 cm^{-1} corresponding to the first overtones ($2\nu_{OH}$) of the structural OH groups and H_2O molecules. The intense band near 5251 cm^{-1} was attributed to the combination mode $(\nu+\delta)_{H_2O}$ of the water molecules and the band at 4533 cm^{-1} to combination modes $(\nu+\delta)_{OH}$ of the structural OH groups (Fig. 10.1.1). Upon acid treatment, the intensities of these bands gradually decreased as a result of the decomposition of the Mt layers. A new band at 7311 cm^{-1} assigned to $2\nu_{SiOH}$ confirmed the creation of SiOH groups (Pálková et al., 2003).

Early acid-dissolution studies, based on solution analysis, of dioctahedral smectites in HCl by Osthaus (1954, 1956) indicated faster dissolution of octahedral than tetrahedral sheets. Assays of solid reaction products employing advanced spectroscopic techniques provided experimental evidence that acid treatments dissolved central atoms from the tetrahedral and octahedral sheets at similar rates (Luca and MacLachlan, 1992; Tkáč et al., 1994).

Luca and MacLachlan (1992) studied the dissolution in 10% HCl of two nontronites from by Mössbauer spectroscopy. They fitted the spectra either with two octahedral Fe^{3+} doublets only, or with an additional tetrahedral Fe^{3+} doublet. Acid treatment appeared to remove octahedral and tetrahedral Fe^{3+} from the structure at about the same rate. Mössbauer and IR spectroscopies and XRD indicated that the remaining undissolved part was the untreated nontronite. ^{27}Al and ^{29}Si MAS-NMR study on removal of tetrahedral and octahedral Al^{3+} from Mt by 6 M HCl led to very similar conclusions (Tkáč et al., 1994). The rates of dissolution of tetrahedral and octahedral Al^{3+} were also comparable. Three different types of structural units were identified in acid-treated samples, including $(SiO)_3SiOH$ units remaining as a result of poor ordering of the framework without the possibility of cross-linking.

The extent of the dissolution reaction depended on both clay mineral type and reaction conditions, such as the acid/clay mineral ratio, acid concentration, time and temperature of the reaction (Komadel, 2003; Sakizci et al., 2011). The composition of the clay mineral layers substantially affected their stability against acid attack; trioctahedral layers dissolved much faster than their dioctahedral counterparts. Higher substitutions of Mg^{2+} and/or Fe^{3+} for Al^{3+} in dioctahedral smectites increased their dissolution rate in acids (Vicente et al., 1994, 1995a; Komadel et al., 1996b; Madejová et al., 1998, 2009b; Steudel et al., 2009a). For 15 dioctahedral smectites, a good correlation of the Mg^{2+} and Fe^{3+} contents was obtained with the half-time of dissolution in 6 M HCl at 96 °C (Novák and Číčel, 1978).

Li^+ dissolved slightly faster than Mg^{2+} from hectorite layers at low acid concentrations (Komadel et al., 1996b). Thus, protons were preferentially attracted by sites close to Li^+ (in the octahedral sheet) that were more negative compared to sites adjacent to Mg^{2+}. This difference disappeared at high acid concentrations when the reaction rates were high. Similarly, octahedrally coordinated Mg^{2+} cations were preferentially released by HCl in comparison with Fe^{3+} and Al^{3+} (Christidis et al., 1997; Gates et al., 2002). The effect of acid anion on dissolution of hectorite is complex and remains uncertain (Komadel et al., 1996b; Van Rompaey et al., 2002). Effects of smectite type, acid concentration and temperature on the half-time of dissolution in 0.2 L HCl/g smectite, acid/clay mineral ratio in closed systems (no substances being added or removed) are summarized in Table 10.1.1. The rate of dissolution of various atoms obtained from chemical analysis of the liquid reaction products indicated the presence of different phases in bentonite. Readily soluble octahedral and tetrahedral constituents and 'insoluble' portions of constituent atoms calculated from the dissolution curves provided information on the distribution of atoms in the sample (Čičel and Komadel, 1994). Readily soluble portions included exchangeable cations and easily soluble admixtures such as goethite (Komadel et al., 1993) and calcite (Komadel et al., 1996b). The most common 'insoluble' phases found in the fine fractions of bentonites were kaolinite, quartz, anatase and volcanic glass. Halloysite was the most decomposed

TABLE 10.1.1 Effects of Smectite Type, Acid Concentration and Temperature on Half-Time of Dissolution in 0.2 L HCl/g Smectite in Closed Systems

Smectite	HCl (M)	T (°C)	$t_{0.5}$ (h)
Effect of smectite type			
Nontronite	6.0	95	0.16
Mg-rich montmorillonite	6.0	95	6.2
Al-rich montmorillonite	6.0	95	8.0
Effect of acid concentration			
Hectorite	0.25	20	4.6
Hectorite	0.50	20	2.6
Hectorite	1.00	20	1.7
Effect of temperature			
Fe^{3+}-beidellite	6.0	50	12.0
Fe^{3+}-beidellite	6.0	60	6.0

mineral after reaction in sulphuric acid of different concentrations, followed by Mt, pyrophyllite and kaolinite (Kato et al., 1966). The observed low dissolution rate of pyrophyllite compared with Mt was due to (i) low octahedral substitution and (ii) the presence of collapsed non-swelling interlayer spaces in pyrophyllite.

Pentrák et al. (2010) investigated the influence of chemical composition and swelling ability of three dioctahedral clay minerals from the Mt-illite series on their dissolution in 6 M HCl. Mt was completely dissolved within 18 h, while the residues of non-decomposed illite could be distinguished in both samples with prevailing non-swelling interlayer spaces, treated for 36 h. Chemical composition of dioctahedral clay minerals had a greater effect on the dissolution rate than swellability. Illite with higher degrees of substitution of Mg^{2+} and Fe^{3+} for Al^{3+} in the octahedral sheets and of Al^{3+} for Si^{4+} in the tetrahedra was more easily soluble in HCl than the illite/smectite with 30% swelling interlayer spaces.

A series of reduced-charge Mt was prepared via Li^{+} fixation at elevated temperatures (the Hofmann–Klemen effect) to explore how the expandability of the interlayer spaces influenced the extent of dissolution. As the negative LC decreased, the content of non-swelling interlayer spaces increased (Komadel et al., 1996a). The dissolution of reduced-charge Mt in HCl indicated that pyrophyllite-like layers surrounded by non-swelling interlayer spaces dissolved more slowly than Mt layers of similar chemical composition located between swelling interlayer spaces (Fig. 10.1.2). This clearly showed that protons attacked the layers from the swollen interlayer spaces also.

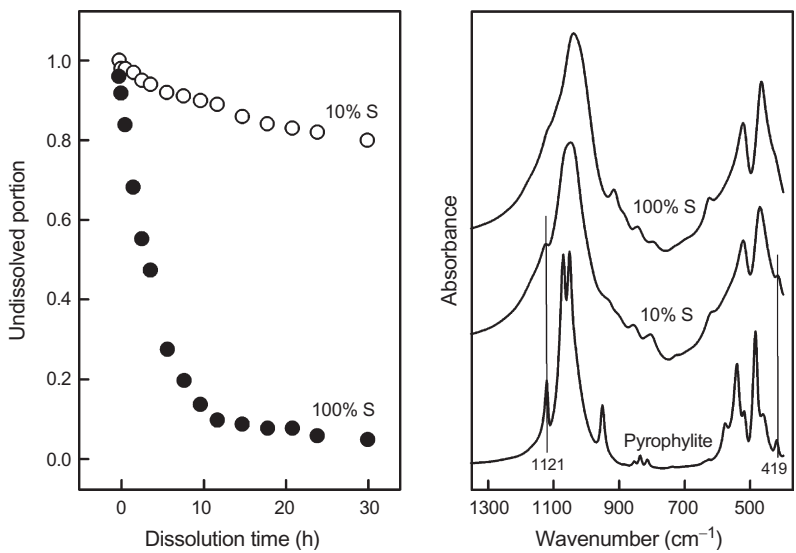

FIGURE 10.1.2 Ca^{2+}-saturated 100% smectite and a reduced-charge smectite with about 10% swelling interlayers. Left: dissolution of Al^{3+} in 6 M HCl at 95 °C; Right: pyrophyllite-like features in the IR spectra. *From Komadel et al. (1996a).*

Non-swelling illite and kaolinite were also more resistant to HCl attack than Mt or vermiculite (Jozefaciuk and Bowanko, 2002).

An *in situ* observation by AFM showed that the dissolution of hectorite and nontronite in acid solutions occurred inward from the edges; the basal surfaces were unreactive. The hectorite (0 1 0) faces dissolved more slowly than the lath ends. The edges dissolved on all sides and roughened. The (010), (110) and (110) faces on nontronite were stable. Dissolution fronts originating at the edges or defects would quickly became fixed along these faces, after which no more dissolution was observable. All the oxygen atoms on the nontronite stable edge faces were saturated, whereas the connecting oxygen atoms on all hectorite edge faces and nontronite edges were coordinatively unsaturated. This difference in reactivity of these faces suggested that the rate-limiting step of the dissolution process was the breaking of the bonds of connecting oxygen atoms (Bickmore et al., 2001).

10.1.4 ACID DISSOLUTION OF ORGANO-SMECTITES

The hydrophilic surface of swelling clay minerals could be rendered hydrophobic by exchanging the naturally occurring inorganic cations with organic (mostly alkylammonium) cations. The size and the amount of organic cations significantly affect the dissolution rate of smectites in acids (Breen et al., 1997a). Both the MIR spectra and the carbon content revealed that only a small proportion of dodecyl- or octadecyl trimethylammonium was displaced during HCl treatment of organo-smectites, and the remaining alkylammonium cations protected the smectite from acid attack. The long-chain alkylammonium cations restricted the access of protons to the layers, and the extent of acid attack was reduced.

Dissolution of organo-smectites in HCl could be effectively followed also by NIR spectroscopy (Madejová et al., 2009b; Tomić et al., 2012). The spectra of SAz-1 Mt saturated with tetramethylammonium (TMA^+) and hexadecyl trimethylammonium ($HDTMA^+$) cations showed the bands related to $2\nu_{OH}$ and $2\nu_{H_2O}$ (7060 cm^{-1}), $(\nu+\delta)_{H_2O}$ (5246 cm^{-1}), and $(\nu+\delta)_{OH}$ (4515 cm^{-1}) as well as the first overtones (6100–5500 cm^{-1}) and combinations modes (4500–4000 cm^{-1}) of CH_3 and CH_2 groups (Fig. 10.1.3; based on the data in Madejová et al., 2009b). The $2\nu_{CH_3}$ region of TMA^+-SAz-1 Mt dissolved for 2 h in 6 M HCl at 80 °C revealed the disappearance of all bands, but the shoulders near 4445 and 4321 cm^{-1} confirmed that not all TMA^+ cations were exchanged by protons. The appearance of a weak $2\nu_{SiOH}$ band at 7316 cm^{-1} substantiated the acidification of the TMA^+-SAz-1 Mt surface. The absence of CH_3 bands, the increased intensity of the $2\nu_{SiOH}$ band, and the reduced intensity of the structural OH overtone band along with the appearance of the $(\nu+\delta)_{SiOH}$ band at 4551 cm^{-1} confirmed that the 6-h dissolution of TMA^+-SAz-1 Mt yielded protonated amorphous silica.

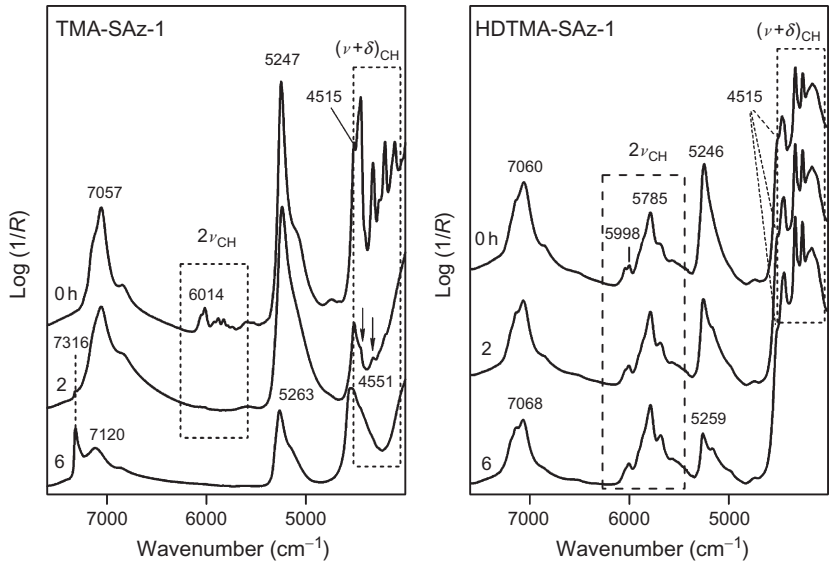

FIGURE 10.1.3 NIR spectra of TMA-SAz-1 Mt and HDTMA-SAz-1 Mt of acid-untreated, and of treated in 6 M HCl at 80 °C for 2 h and 6 h.

In contrast to TMA^+-SAz-1 Mt, the spectrum of $HDTMA^+$-SAz-1 Mt treated in HCl for 2 h showed no sign of the organo-Mt modification (Fig. 10.1.3). After the 6 h treatment, the intensities of the CH_3, CH_2 and OH overtones and combination modes revealed only slight changes of the Mt structure. Moreover, the absence of the Si–OH overtone indicated that large $HDTMA^+$ ions fully covered the inner and outer surfaces of Mt particles and hindered the access of protons to the $Si–O^-$ bonds created by acid activation.

Pálková et al. (2011) and Madejová et al. (2012) investigated the effect of surfactant size on the structure, surface and properties of organo-Mt treated with 6 M HCl at 80 °C. The samples were prepared from SAz-1 Mt and organic cations of progressively increasing alkyl-chain length. While the large plate-like particles of Me_4N^+-Mt were generally disintegrated, the morphology of Bu_4N^+-Mt was only slightly modified. The least stable were Na^+-Mt and Me_4N^+-Mt with a decrease in the content of octahedral atoms to ~5% of the original value after the 8-h treatment. Et_4N^+-Mt and Pr_4N^+-Mt were slightly more resistant mainly to short treatments. Bu_4N^+-Mt and Pe_4N^+-Mt revealed the least structural modifications—only 50% and 35% of octahedral atoms, respectively—were released into solution within the 8-h treatment. IR spectra confirmed the creation of protonated silica in all acid-treated samples including those with a minor decomposition of the structure. This observation indicated that larger Bu_4N^+ and Pe_4N^+ ions created a rather dense organic phase covering the inner and outer surfaces of Mt. This phase hindered the access of protons to the layers and thus protected them from degradation in HCl.

However, the density of packing of these cations and/or their stability in organo-Mt was lower than that of $HDTMA^+$ ions (Madejová et al., 2009b). The accessibility of the interlayer space affected substantially the dissolution of smectites in acids.

10.1.5 PROPERTIES OF ACID-ACTIVATED SMECTITES

10.1.5.1 Layer Charge

Structural modification of smectites upon acid treatment was closely connected with the LC alteration. LC in acid-treated samples was compensated mostly by the protons that had substituted the exchangeable cations. UV–vis spectroscopy of the smectite dispersions with methylene blue (MB) was used for controlling the modification of LC (Madejová et al., 2007; Pentrák et al., 2012). Different dye species, such as the monomers, dimers, H-aggregates and J-aggregates, were adsorbed on the samples as a result of the LC variations. As a consequence of the acid treatment, the amount and/or size of the H-aggregates of MB decreased, while the content of the monomeric forms of adsorbed dye cations increased. The changes in LC observed in the spectra of smectites showed different rates of dissolution in HCl depending on the type of central atoms. The MB spectra of SWy-2 Mt revealed a pronounced heterogeneity of the LC distribution in this low-charge Mt.

The decomposition of the clay mineral structure upon acid or alkaline treatment also modified their variable charge (Jozefaciuk, 2002). Different clay minerals were reacted with HCl or NaOH at room temperature (RT) for 2 weeks. Both treatments increased the variable surface charge, but the actual charge value increased and decreased depending on the mineral and the reaction conditions. Charge-generating surface groups were observed to be heterogeneous. During acid treatment, the number of weakly acidic surface groups increased, while the number of groups of stronger acidic character decreased.

10.1.5.2 Specific Surface Area

The most important physical changes in acid-activated smectites included increase in the SSA and the average pore volume. The extent of these changes depended on the acid strength, time of the treatment and the heating mode. Acid activation of smectites was faster with microwave irradiation than with conventional heating. The SSA and porosity of the samples were similar for comparably dissolved materials (Korichi et al., 2012). A mathematical model incorporating the relationships among time, acid concentration, microwave heating power, and the structural and textural properties of acid-activated bentonite showed that the duration of microwave irradiation was less significant than the other two factors (Petrović et al., 2012).

Acid activation of bentonites caused a splitting of particles within the dissolved octahedral sheets along with an increase in the SSA and decrease in the CEC of the bentonites (Tomić et al., 2011). The SSA of acid-activated samples was several times larger than that of untreated materials. Christidis et al. (1997) reported a four- to fivefold increase in the SSA of two HCl-activated bentonites. After reaching a maximum value (usually under intermediate activation conditions), the SSA decreased with further treatment.

Two saponites and a ferrous saponite (griffithite) were reacted by up to 2.5% HCl at 25 °C for periods up to 48 h. Most of the octahedral sheets of the minerals were dissolved, as was indicated by the high removal of Mg^{2+}, the changes in the IR spectra and the TGA-DTA curves of the activated saponites. Destruction of the saponite structure yielded free silica, and the SSA of the saponites was doubled even after the mild acid activation (Vicente et al., 1996b; Suárez Barrios et al., 2001). The SSA of griffithite samples increased largely after activation, with values up to 10 times higher than the SSA of the untreated sample. The creation of microporosity had a substantial influence on SSA. Likewise, the free silica had a very important contribution to the SSA of leached samples (Vicente et al., 1995b). The high SSA (197 m^2/g) of a natural saponite was related to the very small particle size because of its sedimentary origin. Reaction of sedimentary saponites at RT with 0.62% HCl for times up to 48 h, or by 1.25% HCl solutions for times up to 6 h, produced a partial dissolution of the clay mineral. A mixture of unaltered saponite and free silica was obtained. The solid products consisted mainly of delaminated layers, free silica and insoluble impurities. The SSA was 462 m^2/g and the number of acid centres was 0.98 mmol H^+/g (Prieto et al., 1999).

10.1.5.3 Porous Structure

Textural characteristics such as pore volume or pore size distribution played a significant role in the clay mineral applications. Babaki et al. (2008) reported that the physical and chemical properties of bentonites, such as adsorption and catalytic activity, depended extensively on the micro and mesopores. Though the macropores were accessible between the particles, their effect on the adsorptive properties of a solid was negligible compared to that of the micropores and mesopores located within the particles. Various techniques such as acid treatment or pillaring were used to improve the mesoporosity of smectites.

A short-time synthesis route for preparation of mesoporous materials (folded sheet materials, FSM) was developed from HCl-leached saponite samples. The acid treatment was performed under stirring for 24 h at 25 and 100 °C in 6–10 and 3–7 M HCl solutions. The leached silicate powders were washed and dispersed in HDTMA bromide solution as a structure-directing agent with stirring at pH 12.3 for 3 h at 70 °C and afterwards at pH 8.5 for an additional 3 h at RT, and finally calcined at 550 °C to obtain the

mesoporous materials. A general improvement in the mesoporous FSM structure was obtained when a filtration step was added to the synthesis route after the dissolution at pH 12.3, by removing all dissolved silicates and thus preventing the formation of amorphous silica. The material synthesized after acid leaching by 8 M HCl at RT had the most condensed structure, the highest unit cell dimensions, SSA, and pore volume, and the narrowest pore size distribution (Linssen et al., 2002). The properties of the FSM prepared from differently HCl-treated saponite samples are reported in Table 10.1.2. For most preparations obtained at 25 °C, the BET SSAs were much higher and more sensitive to the acid concentrations than for the materials prepared at 100 °C. The material obtained after leaching with 5 M HCl at 100 °C had the highest pore volume.

Acid activation of a Ca^{2+}-Mt by reaction with sulphuric acid solutions and subsequent pillaring (intercalation of oligomeric Al (hydr)oxides, 'Keggin ions' and calcination at temperatures up to 500 °C) produced new materials for bleaching of cottonseed oil, with the bleaching properties dependent on the extent of activation prior to pillaring. The pillared, acid-activated Mt possessed a higher bleaching efficiency compared to the pillared non-activated clay minerals. Mild activation of the Mt followed by pillaring produced materials with the best fractional degree of bleaching (Falaras et al., 2000b).

A detailed study of the preparation and characterization of Al PILC (see Chapter 10.5) derived from an acid-treated Mt showed that careful selection of the level of acid treatment was necessary to optimize the SSA, pore volume, surface acidity and thermal stability of the final PILC. The optimum level of acid treatment corresponded to the removal of between 19% and

TABLE 10.1.2 Effect of Acid Concentration on BET Specific Surface Areas and Pore Volumes (PV) of Mesoporous FSMs Prepared from Saponite Samples Leached by HCl at 25 and 100 °C

Acid leaching at 25 °C					
HCl (mol/dm^3)	6	7	8	9	10
S_{BET} (m^2/g)	643	726	900	785	478
PV (cm^3/g)	0.44	0.54	0.61	0.54	0.37
Acid leaching at 100 °C					
HCl (mol/dm^3)	3	4	5		
S_{BET} (m^2/g)	521	539	575		
PV (cm^3/g)	0.50	0.45	0.98		

Data from Linssen et al. (2002).

35% of the octahedral cations. However, these values depended on the clay mineral. The previously acid-activated PILC had significantly higher pore volume and acidity than conventional PILC but similar basal spacings, SSA and thermal stability. The higher acidity was mainly due to an increase in Brønsted acid sites arising from the treatment before the pillaring procedure. The higher acidity of the previously acid-activated PILC was reflected in the better catalytic activity for acid-catalyzed reactions as compared with other PILC (Mokaya and Jones, 1995).

Porous clay heterostructures (PCH) with enhanced acidity may be prepared from suitably acid-activated Mt. Their high acidity arose from Brønsted acid sites (Pichowicz and Mokaya, 2001). Kooli et al. (2006) examined the effect of acid activation on the properties of PCH using three Mt of different CEC. A short order in the structure as revealed by the powder XRD of acid-activated PCH was observed, with higher SSA, pore volume and acidity compared to the original clay minerals. The nature of the clay mineral affected the textural properties and the acidity of the prepared porous materials. However, these properties were not enhanced as expected when compared to the PCH.

10.1.5.4 Catalytic Properties

Acid-activated clay minerals were well established as both solid acid catalysts and catalyst supports. The nature of the exchangeable cations substantially affected the acidity of clay mineral catalysts. The high catalytic activity of Al^{3+}-exchanged Mt was attributed to the enhanced polarization of water molecules in the primary coordination sphere around the Al^{3+} ions, which gave rise to strong Brønsted acidity (Varma, 2002; Jankovič and Komadel, 2003b).

H^{+}-saturated Mt of considerable catalytic activity could be prepared by thermal decomposition of ammonium-exchanged clay minerals (Jankovič and Komadel, 2000, 2003a). However, a more typical way was acid activation of clay minerals with a mineral acid. Acid-activated clay minerals are of interest as high-surface-area supports for environmentally benign catalysts. Commercial products are normally reacted with a fixed amount of acid, sufficient to remove the required number of octahedral cations to optimize the SSA and Brønsted acidity for a particular application. However, only a few systematic studies have been reported on how the extent of acid activation of the parent mineral contributes to the catalytic activity.

Several studies have illustrated the application of commercial acid-activated Mt (K-catalysts). Flessner et al. (2001) investigated the surface acidity of a series K-catalysts using a wide range of complementary experimental techniques. The different methods applied allowed a rather complete characterization of the surface acidity. The strength and density of Brønsted acid sites were correlated with the trend in iso-butene conversion. Further activation of K-10 Mt commonly used as a heterogeneous acid catalyst (Wallis

et al., 2007) with HCl of varying concentrations increased its catalytic activity in three test reactions: tetrahydropyranylation of ethanol, diacetylation of benzaldehyde and esterification of succinic anhydride.

The catalytic activity of acid-activated Mt for Brønsted acid-catalyzed reactions was highly dependent on the extent of acid treatment. Two contrasting model reactions were used. The first, involving highly polar reactants, is the acid-catalyzed addition of 3,4-dihydropyran to methanol. The dihydropyran molecule was protonated to give a stabilized carbocation that reacted with methanol to form tetrahydropyranyl ether as the only product. The second reaction, involving a non-polar, hydrophobic reactant was the acid-catalyzed rearrangement of alpha-pinene to camphene. The optimum activation conditions depended on the type of reaction being catalyzed (Rhodes and Brown, 1994).

Acid activation of Ca^{2+}-Mt significantly increased its effectiveness as a support for $ZnCl_2$ Friedel–Crafts alkylation catalysts; optimum treatment conditions were established and there was evidence for a synergistic interaction between the adsorbed salt and the acid-activated clay mineral (Rhodes et al., 1991). Maximum activity was associated with long acid treatment times. Structural characterization by XRD, ^{29}Si MA-NMR spectroscopy, and elemental analysis suggested that the amount of the residual clay mineral in the most active supports was small (Rhodes and Brown, 1992).

Different clay minerals, such as magnesium- or aluminium-rich Mt, a ferruginous smectite, an iron-rich beidellite and a hectorite, were leached with H_2SO_4 or HCl. The extent of activation was controlled by the acid concentration and temperature. The elemental composition of the starting materials did not significantly influence the catalytic reaction of 2,3-dihydropyran and methanol to tetrahydropyranyl ether. The Brønsted acidity and catalytic activity of the activated clay minerals were highest for the samples prepared with the mild acid treatments but decreased with increased leaching of octahedral cations. The acid sites of acid-activated Mt were strong enough to produce tetrahydropyranyl ether in 80% yield. However, the acid-activated hectorite showed no catalytic activity. The octahedral depletion correlated well with the acidity (determined from thermal desorption of cyclohexylamine) and the catalytic activity for the chosen test reaction (Breen et al., 1995a,b, 1997b; Komadel et al., 1997).

The catalytic activity for the dimerization of oleic acid increased after mild activation of Mt in HCl. However, the activity of the activated Mt with about 50% of octahedral Al^{3+} removed was comparable to that of the untreated clay mineral (Čičel et al., 1992). Acid-activated smectites can convert alkenes formed by thermal decomposition of high-density polyethylene into light gases and aromatic species. Total conversion increased with both the extent of acid treatment and the temperature. The proportion of aromatic products was largest for catalysts prepared using short acid activation periods (Breen et al., 2000). Acid-activated bentonite (and kaolin) debutylated

2-*tert*-butylphenol and showed varying debutylation versus isomerization selectivity. The resulting catalytic activity of these samples was dependent on the type of acid used. Samples activated with acetic acid showed relatively low conversions, whereas those treated with hydrochloric or phosphoric acids were very active catalysts (Mahmoud and Saleh, 1999).

Acid activation of tetralkylammonium smectites produced hybrid catalysts for the isomerization of alpha-pinene to camphene. This catalytic activity was attributed to the enhanced hydrophobicity of the organo-smectites. Acid-activated TMA^+-smectites were the most active catalysts and yielded 60–90% conversion based on alpha-pinene. The yields were comparable with those obtained with other solid catalysts such as zeolites and PILC. The iron-substituted smectites were more active than their aluminium counterparts. The dodecyl- and octadecyl trimethylammonium smectites were generally less active (Breen et al., 1997a).

SWy-2 Mt and SAz-1 Mt loaded with increasing amounts of the polycation magnafloc were reacted with 6 M HCl at 95 °C. These smectites were active catalysts for the isomerization of alpha-pinene to camphene and limonene. The conversion by the polycation-exchanged SAz-1 Mt was larger than by the unloaded activated counterpart because the former material was more hydrophobic. In the case of SWy-2 Mt, the yields in the absence and presence of polycations were similar, suggesting good dispersion of both samples in the non-polar alpha-pinene. The yields, based on alpha-pinene, for the most active catalysts were between 80% and 90%. These yields were directly comparable to those obtained by using zeolites and PILC, although the acid-activated polycation-treated clay minerals were marginally less selective towards camphene (Breen and Watson, 1998).

Two STx-1 and SWy-2 Mt were activated with different amounts of 12 M HCl and then exchanged with a fixed amount of 1 M TMA^+ chloride solution at RT, giving rise to H^+/TMA^+ Mts. In addition, TMA^+/H^+ samples were obtained by acid activation of TMA^+-exchanged Mt. The acidity was determined by adsorption of cyclohexylamine and the catalytic activity by the isomerization of 1-butene at 300 °C to yield *cis*- and *trans*-2-butene. The total conversion for the isomerization of 1-butene was higher for the TMA^+/H^+ samples than for the H^+/TMA^+ catalysts. TMA^+ cations adsorbed on the clay minerals were extremely resistant to exchange by protons, but protons were easily displaced by TMA^+ cations (Moronta et al., 2002).

10.1.6 ACID DISSOLUTION OF NON-SWELLING CLAY MINERALS

Acid dissolution of non-swelling clay minerals such as illites, kaolinites or fibrous clay minerals (sepiolite and palygorskite) was a widely studied method for improving their surface and catalytic properties (Cai et al., 2007;

Lenarda et al., 2007; Steudel et al., 2009b; Bibi et al., 2011; Valášková et al., 2011; Worasith et al., 2011; Yanik et al., 2012).

10.1.6.1 Kaolinite and Metakaolinite

Dissolution rates of natural kaolinites of different origins, of halloysite and of illitic clays in H_2SO_4 and HCl, were determined by measuring the release rate of aluminium. The dissolution rate of kaolinite in 0.5 M H_2SO_4 at 25 °C was approximately three times higher than in HCl of equivalent proton concentration. The dissolution in 5 M H_2SO_4 was eight times faster when the solid phase was periodically separated from the acid solution, washed with distilled water and dried. The aluminium release rate decreased as the amount of clay-size micas in kaolinitic clays increased. The rate was also affected by the crystallinity of the clay mineral (Hradil et al., 2002). The dissolution process of less ordered kaolinite was increased not only in HCl but also in KOH solutions (Pentrák et al., 2009).

The solubility of kaolinite in acids varied with the nature and concentration of the acid, the acid-to-kaolinite ratio, the temperature and the duration of treatment. The reaction of natural kaolin refluxed with 1–10 M H_2SO_4 at 110 °C for 4 h followed by calcination at 500 °C for 2 h yielded amorphous silica. Leaching of Al^{3+} ions was enhanced progressively with the severity of the acid attack. The acid treatment increased the Si/Al ratio from 0.65 to 8.09, the SSA from 23 to 143 m^2/g and the pore volume from 0.361 to 1.18 cm^3/g when the acid concentration was increased to 10 M. The solids phases thus obtained were used as promising adsorbents and catalyst supports (Panda et al., 2010).

Proton adsorption or desorption might be computed from potentiometric titration data at pH 2–12 using surface complexation models. The pH of zero proton charge was close to 5.5. The positive charge that developed below pH 5.5 was due to proton adsorption on aluminium sites of the octahedral sheet. The external hydroxyl groups of the octahedral sheet were the first to be protonated, whereas the second protonation might take place either at the inner hydroxyl groups or at the edge aluminol groups. Above pH 5.5, the kaolinite surface underwent two successive deprotonations; the first occurred at pH about 5.5 and the second at pH about 9 (Huertas et al., 1998). The dissolution mechanism of kaolinite was mainly controlled by aluminol surface sites (external and internal structural hydroxyl groups and aluminol groups at the particle edges) under both acidic and alkaline conditions (Huertas et al., 1999).

Kaolinite dissolution rates at pH 2–4 and temperatures of 25, 50 and 70 °C were obtained using stirred and non-stirred flow-through reactors. The rates increased with increasing stirring speed, and the stirring effect was reversible. The effect of stirring speed on kaolinite dissolution rate was higher at 25 °C than at 50 and 70 °C and at pH 4 than at pH 2 and 3. Stirring induced formation of fine particles. The ratio of reactive surface area to SSA increased, and

the dissolution rate of kaolinite enhanced. A balance between the production and dissolution of the fine particles explained the reversibility as well as the temperature and the pH dependence of the stirring effect (Metz and Ganor, 2001).

Pyridine and NH_3 adsorption indicated that the strong acid sites on activated kaolinite were of the Lewis type (Tabak and Afsin, 2001). Acid activation increased the protonated species on a kaolinite surface at the expense of coordinately bound NH_3. The presence of NH_4^+ ions on an activated sample did not prove the presence of protonic acid sites alone, since the added protons might have come from the residual water in the interlayer space. Progressive dehydration of the surface resulted in a strong increase in chemisorbed NH_3.

The solid acid-activated metakaolinites are promising as adsorbents and catalyst supports. Metakaolinites were prepared by calcination of kaolinites at 600–900 °C and were more reactive than the parent kaolinite after acid activation with 6 M HCl at 90 °C. Reaction during 6 h removed most of the octahedral Al^{3+} cations and yielded amorphous silica phase with high SSA. Acid treatment for 24 h also removed the octahedral cations, but led to the formation of amorphous silica with much lower SSA. Metakaolinite prepared by calcination at 900 °C had a lower reactivity than the materials obtained at lower temperatures (Belver et al., 2002).

The activated metakaolinites were active catalysts for the alkylation of benzene with benzyl chloride, giving >75% conversion of the alkylating agent. Metakaolinite activated with 4 M HNO_3 led to 87% conversion of benzyl chloride to diphenylmethane with 100% selectivity within 30 min of reaction time. This might be correlated with the greater surface acidity of this sample. Extremely efficient solid catalysts of remarkable acidic properties could be produced by the activation of metakaolinite with H_2SO_4, HNO_3 and $HClO_4$ (Sabu et al., 1999).

10.1.6.2 Sepiolite and Palygorskite

Sepiolite and palygorskite, the fibrous clay minerals, have wide-ranging industrial and medical applications, particularly as adsorbents, catalysts or catalyst supports because of their structural characteristics and physicochemical properties. Heating and acid activation are often used to enhance their properties (Valentín et al., 2007). Acid activation of palygorskite followed by *in situ* hydrothermal treatment was successfully utilized in zeolite A synthesis (Jiang et al., 2012).

When sepiolite and palygorskite were activated by HCl, the octahedral sheets progressively dissolved. The content of silica increased and that of octahedral cations decreased with the intensity of the acid attack. In both cases, fibrous free silica was obtained. Sepiolite decomposed more rapidly than palygorskite because its octahedral sheets contain more Mg^{2+} and the structural micro-channels are larger. The removal of the cations and

disaggregation of the particles, as well as the increase in the micropore volume, enlarged the SSA (Myriam et al., 1998). A substantial increase in the SSA was also observed for HCl-treated palygorskite. The free silica obtained had the fibrous morphology of natural palygorskite, but no microporosity was detected (Suárez Barrios et al., 1995).

After dissolution of sepiolite samples in HCl, the free silica produced had little influence on the properties of the mildly acid-treated solids. However, the influence of this silica became important when solids were obtained by more intense treatments (Vicente et al., 1995b). As the amount of iron and aluminium extracted from sepiolite increased, the SSA of the mineral grew from 195 to 306 m^2/g and the original microporous structure became mesoporous.

The CEC of sepiolite could be fully eliminated by acid treatment, during which the mineral structure was progressively transformed into amorphous silica–alumina (Dekany et al., 1999). The BET surface area of the original sepiolite increased from 148 to 263 m^2/g and decreased afterwards. Approximately 16% of the total volume was in the micropores. Acid activation restricted particle deformation during thermal treatment. The micropore volume increased by 20% and the BET surface area reached values >500 m^2/g for the acid-treated samples (Balci, 1999).

Natural and acid-activated sepiolites and palygorskites are often used as adsorbents for the removal of heavy metals from aqueous solutions (Chen et al., 2007; Wang et al., 2007). Frini-Srasra and Srasra (2010) reported a pronounced increase in the SSA of HCl-treated Tunisian palygorskite due to dissolution of octahedral sheets and the creation of mesoporosity. The acid-activated samples showed a higher adsorption capacity for Cd^{2+} than the natural palygorskite.

10.1.7 CONCLUSION

Acid activation of clays and clay minerals has been used for decades both in laboratories for basic and applied research and in industrial production for many applications. Even so, it remains one of the most common chemical modifications of clays and clay minerals for the future of clay science and applications.

REFERENCES

Adams, J.M., 1987. Synthetic organic chemistry using pillared, cation-exchanged and acid-treated montmorillonite catalysts—a review. Appl. Clay Sci. 2, 309–342.

Babaki, H., Salem, A., Jafarizad, A., 2008. Kinetic model for the isothermal activation of bentonite by sulfuric acid. Mater. Chem. Phys. 108, 263–268.

Balci, S., 1999. Effect of heating and acid pre-treatment on pore size distribution of sepiolite. Clay Miner. 34, 647–655.

Barshad, I., Foscolos, A.E., 1970. Factors affecting the rate of interchange reaction of adsorbed H^+ on the 2:1 clay minerals. Soil Sci. 110, 52–60.

Belver, C., Bañares Muñoz, M.A., Vicente, M.A., 2002. Chemical activation of a kaolinite under acid and alkaline conditions. Chem. Mater. 14, 501–506.

Bibi, I., Singh, B., Silvester, E., 2011. Dissolution of illite in saline-acidic solutions at 25 degrees C. Geochim. Cosmochim. Acta 75, 3237–3249.

Bickmore, B.R., Bosbach, D., Hochella, M.F., Charlet, L., Rufe, E., 2001. In situ atomic force microscopy study of hectorite and nontronite dissolution: implications for phyllosilicate edge surface structures and dissolution mechanisms. Am. Mineral. 86, 411–423.

Bovey, J., Jones, W., 1995. Characterisation of Al-pillared acid-activated clay catalysts. J. Mater. Chem. 5, 2027–2035.

Bovey, J., Kooli, F., Jones, W., 1996. Preparation and characterization of Ti-pillared acid-activated clay catalyst. Clay Miner. 31, 501–506.

Breen, C., Watson, R., 1998. Acid-activated organoclays: preparation, characterisation and catalytic activity of polycation-treated bentonites. Appl. Clay Sci. 12, 479–494.

Breen, C., Madejová, J., Komadel, P., 1995a. Correlation of catalytic activity with infrared-red, ^{29}Si MAS NMR and acidity data for HCl-treated fine fractions of montmorillonites. Appl. Clay Sci. 10, 219–230.

Breen, C., Madejová, J., Komadel, P., 1995b. Characterisation of moderately acid-treated, size-fractionated montmorillonites using IR and MAS NMR spectroscopy and thermal analysis. J. Mater. Chem. 5, 469–474.

Breen, C., Zahoor, F.D., Madejová, J., Komadel, P., 1997a. Characterisation and catalytic activity of acid treated, size fractionated smectites. J. Phys. Chem. B 101, 5324–5331.

Breen, C., Watson, R., Madejová, J., Komadel, P., Klapyta, Z., 1997b. Acid-activated organoclays: preparation, characterisation and catalytic activity of acid-treated tetra-alkylammonium exchanged smectites. Langmuir 13, 6473–6479.

Breen, C., Last, P.M., Taylor, S., Komadel, P., 2000. Synergic chemical analysis—the coupling of TG with FTIR, MS and GC-MS 2. Catalytic transformation of the gases evolved during the thermal decomposition of HDPE using acid-activated clays. Thermochim. Acta 363, 93–104.

Brown, D.R., 1994. Review: clays as catalyst and reagent supports. Geol. Carpath. Ser. Clays 45, 45–56.

Cai, Y.F., Xue, J.Y., Polya, D.A., 2007. A Fourier transform infrared spectroscopic study of Mg-rich, Mg-poor and acid leached palygorskites. Spectrochim. Acta A 66, 282–288.

Carrado, K.A., Komadel, P., 2009. Acid activation of bentonites and polymer-clay nanocomposites. Elements 5, 111–116.

Chen, H., Zhaoa, Y., Wang, A., 2007. Removal of Cu(II) from aqueous solution by adsorption onto acid-activated palygorskite. J. Hazard. Mater. 149, 346–354.

Christidis, G.E., Scott, P.W., Dunham, A.C., 1997. Acid activation and bleaching capacity of bentonites from the islands of Milos and Chios, Aegean, Greece. Appl. Clay Sci. 12, 329–347.

Čičel, B., Komadel, P., 1994. Structural formulae of layer silicates. In: Amonette, J.E., Zelazny, L.W. (Eds.), Quantitative Methods in Soil Mineralogy. Soil Science Society of America Miscellaneous Publication, Madison, WI, pp. 114–136. Soil Science Society of America.

Čičel, B., Komadel, P., Nigrin, M., 1992. Catalytic activity of smectites on dimerization of oleic acid. Collect. Czech. Chem. Commun. 57, 1666–1671.

Dekany, I., Turi, L., Fonseca, A., Nagy, J.B., 1999. The structure of acid treated sepiolites: small-angle X-ray scattering and multi MAS-NMR investigations. Appl. Clay Sci. 14, 141–160.

Dubíková, M., Cambier, P., Šucha, V., Čaplovičová, M., 2002. Experimental soil acidification. Appl. Geochem. 17, 245–257.

Fahn, R., Fenderl, K., 1983. Reaction products of organic dye molecules with acid-treated montmorillonite. Clay Miner. 18, 447–458.

Falaras, P., Kovanis, I., Lezou, F., Seiragakis, G., 1999. Cottonseed oil bleaching by acid-activated montmorillonite. Clays Clay Miner. 34, 221–232.

Falaras, P., Lezou, F., Pomonis, P., Ladavos, A., 2000a. Al-pillared acid-activated montmorillonite modified electrodes. J. Electroanal. Chem. 486, 156–165.

Falaras, P., Lezou, F., Seiragakis, G., Petrakis, D., 2000b. Bleaching properties of alumina-pillared acid-activated montmorillonite. Clays Clay Miner. 48, 549–556.

Flessner, U., Jones, D.J., Roziere, J., Zajac, J., Storaro, L., Lenarda, M., Pavan, M., Jimenez-Lopez, A., Rodriguez-Castellon, E., Trombetta, M., Busca, G., 2001. A study of the surface acidity of acid-treated montmorillonite clay catalysts. J. Mol. Catal. A Chem. 168, 247–256.

Frini-Srasra, N., Srasra, E., 2010. Acid treatment of south Tunisian palygorskite: removal of Cd(II) from aqueous and phosphoric acid solutions. Desalination 250, 26–34.

Galán, E., Carretero, M.I., Fernandez-Caliani, J.C., 1999. Effects of acid mine drainage on clay minerals suspended in the Tinto River (Rio Tinto, Spain). An experimental approach. Clay Miner. 34, 99–108.

Gates, W.P., Anderson, J.S., Raven, M.D., Churchman, G.J., 2002. Mineralogy of a bentonite from Miles, Queensland, Australia and characterisation of its acid activation products. Appl. Clay Sci. 20, 189–197.

He, H.P., Guo, J.G., Xie, X.D., Lin, H.F., Li, L.Y., 2002. A microstructural study of acid-activated montmorillonite from Choushan, China. Clay Miner. 37, 337–344.

Hradil, D., Hostomský, J., Soukupová, J., 2002. Aluminium release rates from acidified clay structures: comparative kinetic study. Geol. Carpath. 53, 117–121.

Huertas, F.J., Chou, L., Wollast, R., 1998. Mechanism of kaolinite dissolution at room temperature and pressure. Part I: surface speciation. Geochim. Cosmochim. Acta 62, 417–431.

Huertas, F.J., Chou, L., Wollast, R., 1999. Mechanism of kaolinite dissolution at room temperature and pressure. Part II: kinetic study. Geochim. Cosmochim. Acta 63, 3261–3275.

Hussin, F., Aroua, M.K., Daud, W.M.A.W., 2011. Textural characteristics, surface chemistry and activation of bleaching earth: a review. Chem. Eng. J. 170, 90–106.

Janek, M., Komadel, P., 1993. Autotransformation of H-smectites in aqueous solution. Effect of octahedral iron content. Geol. Carpath. Ser. Clays 44, 59–64.

Janek, M., Komadel, P., 1999. Acidity of proton saturated and autotransformed smectites characterised with proton affinity distribution. Geol. Carpath. 50, 373–378.

Janek, M., Lagaly, G., 2001. Proton saturation and rheological properties of smectite dispersions. Appl. Clay Sci. 19, 121–130.

Janek, M., Komadel, P., Lagaly, G., 1997. Effect of autotransformation on the layer charge of smectites determined by the alkylammonium method. Clay Miner. 32, 623–632.

Jankovič, Ľ., Komadel, P., 2000. Catalytic properties of a heated ammonium-saturated dioctahedral smectite. Coll. Czech. Chem. Commun. 65, 1527–1536.

Jankovič, Ľ., Komadel, P., 2003a. Metal cation-exchanged montmorillonite catalysed protection of aromatic aldehydes with Ac_2O. J. Catal. 218, 227–233.

Jankovič, Ľ., Komadel, P., 2003b. Microwave assisted synthesis of substituted indoles using montmorillonite as catalyst. Solid State Phenom. 90–91, 481–486.

Jiang, J.L., Feng, L.D., Gu, X., Qian, Y.H., Gu, Y.X., Duanmu, C.S., 2012. Synthesis of zeolite A from palygorskite via acid activation. Appl. Clay Sci. 55, 108–113.

Jozefaciuk, G., 2002. Effect of acid and alkali treatments on surface-charge properties of selected minerals. Clays Clay Miner. 50, 647–656.

Jozefaciuk, G., Bowanko, G., 2002. Effect of acid and alkali treatments on surface areas and adsorption energies of selected minerals. Clays Clay Miner. 50, 771–783.

Kato, C., Suzuki, T., Fujiwaraa, T., 1966. Decomposition and structural change of clay minerals by acid. Memories of the School of Science and Engineering, Waseda University, pp. 13–24.

Kendall, T., 1996. Smectite clays. In: Kendall, T. (Ed.), Industrial Clays. Industrial Minerals Information Ltd., London, pp. 1–12.

Klika, Z., Pustková, P., Dudová, M., Čapková, P., Kliková, C., Grygar, T.M., 2011. The adsorption of methylene blue on montmorillonite from acid solutions. Clay Miner. 46, 461–471.

Komadel, P., 1999. Structure and chemical characteristics of modified clays. In: Misealides, P., Macášek, F., Pinnavaia, T.J., Colella, C. (Eds.), Natural Microporous Materials in Environmental Technology. Kluwer, The Netherlands, pp. 3–18.

Komadel, P., 2003. Chemically modified smectites. Clay Miner. 38, 127–138.

Komadel, P., Schmidt, D., Madejová, J., Čičel, B., 1990. Alteration of smectites by treatments with hydrochloric acid and sodium carbonate solutions. Appl. Clay Sci. 5, 113–122.

Komadel, P., Stucki, J.W., Čičel, B., 1993. Readily HCl-soluble iron in the fine fractions of some Czech bentonites. Geol. Carpath. Ser. Clays 44, 11–16.

Komadel, P., Bujdák, J., Madejová, J., Šucha, V., Elsass, F., 1996a. Effect of non-swelling layers on the dissolution of reduced-charge montmorillonite in hydrochloric acid. Clay Miner. 31, 333–345.

Komadel, P., Madejová, J., Janek, M., Gates, W.P., Kirkpatrick, R.J., Stucki, J.W., 1996b. Dissolution of hectorite in inorganic acids. Clays Clay Miner. 44, 228–236.

Komadel, P., Janek, M., Madejová, J., Weekes, A., Breen, C., 1997. Acidity and catalytic activity of mildly acid-treated Mg-rich montmorillonite and hectorite. J. Chem. Soc. Faraday Trans. 93, 4207–4210.

Kooli, F., Hian, P.C., Weirong, Q., Alshahateet, S.F., Chen, F., 2006. Effect of the acid-activated clays on the properties of porous clay heterostructures. J. Porous Mater. 13, 319–324.

Korichi, S., Elias, A., Mefti, A., Bensmaili, A., 2012. The effect of microwave irradiation and conventional acid activation on the textural properties of smectite: comparative study. Appl. Clay Sci. 59–60, 76–83.

Lagaly, G., 1994. Layer charge determination by alkylammonium ions. In: Mermut, A.R. (Ed.), Layer Charge Characteristics of 2:1 Silicate Clay Minerals. Clay Minerals Society Workshop Lectures 6, Boulder, CO, USA, pp. 1–46.

Lambert, J.-F., Poncelet, G., 1997. Acidity in pillared clays: origin and catalytic manifestations. Top. Catal. 4, 43–56.

Lenarda, M., Storaro, L., Talona, A., Moretti, E., Riello, P., 2007. Solid acid catalysts from clays: preparation of mesoporous catalysts by chemical activation of metakaolin under acid conditions. J. Colloid Interface Sci. 311, 537–543.

Linssen, T., Cool, P., Baroudi, M., Cassiers, K., Vansant, E.F., Lebedev, O., Van Landuyt, J., 2002. Leached natural saponite as the silicate source in the synthesis of aluminosilicate hexagonal mesoporous materials. J. Phys. Chem. B 106, 4470–4476.

Luca, V., MacLachlan, D.J., 1992. Site occupancy in nontronite studied by acid dissolution and Mössbauer spectroscopy. Clays Clay Miner. 40, 1–7.

Madejová, J., Bujdák, J., Janek, M., Komadel, P., 1998. Comparative FT-IR study of the structural modifications during acid treatment of dioctahedral smectites and hectorite. Spectrochim. Acta A 54, 1397–1406.

Madejová, J., Andrejkovičová, S., Bujdák, J., Čeklovský, A., Hrachová, J., Valúchová, J., Komadel, P., 2007. Characterization of products obtained by acid-leaching of Fe-bentonite. Clay Miner. 42, 527–540.

Madejová, J., Pentrák, M., Pálková, H., Komadel, P., 2009a. Near-infrared spectroscopy: a powerful tool in studies of acid treated clay minerals. Vib. Spectrosc. 49, 211–218.

Madejová, J., Pálková, H., Pentrák, M., Komadel, P., 2009b. Near-infrared spectroscopic analysis of acid-treated organo-clays. Clays Clay Miner. 57, 392–403.

Madejová, J., Pálková, H., Jankovič, Ľ., 2012. Degradation of surfactant-modified montmorillonites in HCl. Mater. Chem. Phys. 134, 768–776.

Mahmoud, S., Saleh, S., 1999. Effect of acid activation on the de-tert-butylation activity of some Jordanian clays. Clays Clay Miner. 47, 481–486.

Metz, V., Ganor, J., 2001. Stirring effect on kaolinite dissolution rate. Geochim. Cosmochim. Acta 65, 3475–3490.

Mokaya, R., Jones, W., 1994. Pillared acid-activated clay catalysts. J. Chem. Soc. Chem. Commun. 1994, 929–930.

Mokaya, R., Jones, W., 1995. Pillared clays and pillared acid-activated clay: a comparative study of physical, acidic and catalytic properties. J. Catal. 153, 76–85.

Mokaya, R., Jones, W., Davies, W., Whittle, M.E., 1993. Preparation of alumina-pillared acid-activated clays and their use as chlorophyll adsorbents. J. Mater. Chem. 3, 381–387.

Moronta, A., Ferrer, V., Quero, J., Arteaga, G., Choren, E., 2002. Influence of preparation method on the catalytic properties of acid-activated tetramethylammonium-exchanged clays. Appl. Catal. Gen. 230, 127–135.

Myriam, M., Suarez, M., Martin-Pozas, J.M., 1998. Structural and textural modifications of palygorskite and sepiolite under acid treatment. Clays Clay Miner. 46, 225–231.

Novák, I., Číčel, B., 1978. Dissolution of smectites in hydrochloric acid: II. Dissolution rate as a function of crystallochemical composition. Clays Clay Miner. 26, 341–344.

Osthaus, B.B., 1954. Chemical determination of tetrahedral ions in nontronite and montmorillonite. Clays Clay Miner. 2, 404–417.

Osthaus, B.B., 1956. Kinetic studies on montmorillonite and nontronite by the acid dissolution technique. Clays Clay Miner. 4, 301–321.

Pagano, T., Sergio, M., Glisenti, L., Diano, W., Grompone, M.A., 2001. Use of pillared montmorillonites to eliminate chlorophyll from rice bran oil. Ing. Quim. 11–19.

Pálková, H., Madejová, J., Righi, D., 2003. Acid dissolution of reduced-charge Li- and Ni-montmorillonites. Clays Clay Miner. 51, 133–142.

Pálková, H., Jankovič, Ľ., Zimowska, M., Madejová, J., 2011. Alterations of the surface and morphology of tetraalkyl-ammonium modified montmorillonites upon acid treatment. J. Colloid Interface Sci. 363, 213–222.

Panda, A.K., Mishraa, B.G., Mishrac, D.K., Singha, R.K., 2010. Effect of sulphuric acid treatment on the physico-chemical characteristics of kaolin clay. Colloids Surf. A Physicochem. Eng. Asp. 363, 98–104.

Pentrák, M., Madejová, J., Komadel, P., 2009. Acid and alkali treatments of kaolins. Clay Miner. 44, 507–519.

Pentrák, M., Madejová, J., Komadel, P., 2010. Effect of chemical composition and swelling on acid dissolution of 2:1 clay minerals. Philos. Mag. 90, 2387–2397.

Pentrák, M., Czímerová, A., Madejová, J., Komadel, P., 2012. Changes in layer charge of clay minerals upon acid treatment as obtained from their interactions with methylene blue. Appl. Clay Sci. 55, 100–107.

Petrović, S., Rožić, L., Vuković, Z., Novaković, T., Stanisavljev, D., 2012. Response surface optimization for activation of bentonite using microwave irradiation. Clays Clay Miner. 60, 32–39.

Pichowicz, M., Mokaya, R., 2001. Porous clay heterostructures with enhanced acidity obtained from acid-activated clays. Chem. Commun. 2001, 2100–2101.

Prieto, O., Vicente, M.A., Bañares-Muñoz, M.A., 1999. Study of the porous solids obtained by acid treatment of a high surface area saponite. J. Porous Mater. 6, 335–344.

Ramesh, S., Bhati, Y.S., Jai Prakash, B.S., 2012. Microwave-activated p-TSA dealuminated montmorillonite—a new material with improved catalytic activity. Clay Miner. 47, 231–242.

Rhodes, C.N., Brown, D.R., 1992. Structural characterization and optimization of acid-treated montmorillonite and high-porosity silica supports for $ZnCl_2$ alkylation catalysts. J. Chem. Soc. Faraday Trans. 88, 2269–2274.

Rhodes, C.N., Brown, D.R., 1994. Catalytic activity of acid-treated montmorillonite in polar and nonpolar reaction media. Catal. Lett. 24, 285–291.

Rhodes, C.N., Franks, M., Parkes, G.M.B., Brown, D.R., 1991. The effect of acid treatment on the activity of clay supports for $ZnCl_2$ alkylation catalysts. J. Chem. Soc. Chem. Commun. 12, 804–807.

Sabu, K.R., Sukumar, R., Rekha, R., Lalithambika, M., 1999. A comparative study on H_2SO_4, HNO_3 and $HClO_4$ treated metakaolinite of a natural kaolinite as Friedel-Crafts alkylation catalyst. Catal. Today 49, 321–326.

Sakizci, M., Erdoğan Alver, B., Yörükoğulları, E., 2011. SO_2 adsorption on acid-treated bentonites from Turkey. Clay Miner. 46, 73–83.

Scarletti, N.V.Y., Raven, M., Madsen, I., 2011. Powder X-ray diffraction study of the hydration and leaching behavior of nontronite. Clays Clay Miner. 59, 560–567.

Siddiqui, M.H.K., 1968. Bleaching Earths. Pergamon Press, London, 86 pp.

Steudel, A., Batenburg, L.H., Fischer, H.R., Weidler, P.G., Emmerich, K., 2009a. Alteration of swelling clay minerals by acid activation. Appl. Clay Sci. 44, 105–115.

Steudel, A., Batenburg, L.H., Fischer, H.R., Weidler, P.G., Emmerich, K., 2009b. Alteration of non-swelling clay minerals and magadiite by acid activation. Appl. Clay Sci. 44, 95–104.

Suárez Barrios, M., Flores González, L.V., Vicente, M.A., Martín Pozas, J.M., 1995. Acid activation of palygorskite with HCl: development of physico-chemical textural and surface properties. Appl. Clay Sci. 10, 247–258.

Suárez Barrios, M., Buey, C.S., Garcia Romero, E., Martín Pozas, J.M., 2001. Textural and structural modifications of saponite from Cerro del Aguila by acid treatment. Clay Miner. 36, 483–488.

Tabak, A., Afsin, B., 2001. Firmly adsorbed ammonia and pyridine species at activated kaolinite surfaces. Adsorpt. Sci. Technol. 19, 673–679.

Tkáč, I., Komadel, P., Müller, D., 1994. Acid-treated montmorillonites—a study by ^{29}Si and ^{27}Al MAS-NMR. Clay Miner. 29, 11–19.

Tomić, Z., Logar, V.P., Babic, B.M., Rogan, J.R., Makreski, P., 2011. Comparison of structural, textural and thermal characteristics of pure and acid treated bentonites from Aleksinac and Petrovac (Serbia). Spectrochim. Acta A 82, 389–395.

Tomić, Z., Ašanin, D., Antić-Mladenović, S., Poharc-Logar, V., Makreski, P., 2012. NIR and MIR spectroscopic characteristics of hydrophilic and hydrophobic bentonite treated with sulphuric acid. Vib. Spectrosc. 58, 95–103.

Valášková, M., Barabaszová, K., Hundaková, M., Ritz, M., Plevová, E., 2011. Effects of brief milling and acid treatment on two ordered and disordered kaolinite structures. Appl. Clay Sci. 54, 70–76.

Valentín, J.L., Lopéz-Manchado, M.A., Rodríguez, A., Posadas, P., Ibarra, L., 2007. Novel anhydrous unfolded structures by heating of acid pre-treated sepiolite. Appl. Clay Sci. 36, 245–255.

Van Rompaey, K., Van Ranst, E., De Coninck, F., Vindevogel, N., 2002. Dissolution characteristics of hectorite in inorganic acids. Appl. Clay Sci. 21, 241–256.

Varma, R.S., 2002. Clay and clay-supported reagents in organic synthesis. Tetrahedron 58, 1235–1255.

Vicente, M.A., Suárez Barrios, M., López-González, J.D., Bañares-Muñoz, M.A., 1994. Acid activation of a ferrous saponite (griffithite): physicochemical characterization and surface area of the products obtained. Clays Clay Miner. 42, 724–730.

Vicente, M.A., López González, J.D., Bañares Muñoz, M.A., 1995a. Preparation of microporous solids by acid treatment of a saponite. Microporous Mater. 4, 251–264.

Vicente, M.A., Lopez-González, J.D., Bañares-Muñoz, M.A., 1995b. Influence of the free silica generated during acid activation of a sepiolite on adsorbent and textural properties of the resulting solids. J. Mater. Chem. 5, 127–132.

Vicente, M.A., Suárez, M., Bañares Muñoz, M.A., López González, J.D., 1996a. Comparative FT-IR study of the removal of octahedral cations and structural modifications during acid treatment of several silicates. Spectrochim. Acta A 52, 1685–1694.

Vicente, M.A., Suárez Barrios, M., López-González, J.D., Bañares-Muñoz, M.A., 1996b. Characterization, surface area, and porosity analyses of the solids obtained by acid leaching of a saponite. Langmuir 12, 566–572.

Wallis, P.J., Gates, W.P., Patti, A.F., Scott, J.L., Teoh, R., 2007. Assessing and improving the catalytic activity of K-10 montmorillonite. Green Chem. 9, 980–986.

Wang, W., Chen, H., Wang, A., 2007. Adsorption characteristics of Cd(II) from aqueous solution onto activated palygorskite. Sep. Purif. Technol. 55, 157–164.

Worasith, N., Goodman, B.A., Neampan, J., Jeyachoke, N., Thiravetyani, P., 2011. Characterization of modified kaolin from the Ranong deposit Thailand by XRD, XRF, SEM, FTIR and EPR techniques. Clay Miner. 46, 539–559.

Yanik, G., Cleylantekin, R., Tasci, E., Ozcay, U., 2012. The Sahin village (Kutahya, Turkey) clay deposit and its possible utilization. Clay Miner. 47, 1–10.

Zysset, M., Schindler, W., 1996. The proton promoted dissolution kinetics of K-montmorillonite. Geochim. Cosmochim. Acta 60, 921–931.